

thermoplastics, there are no catalyst residues in these polymers. The products are exceptionally pure as a result of the biosynthetic process and solvent-based extraction and purification procedures. The major impurities are inorganic nitrogen, phosphorous and sulphur-containing compounds which are present at concentrations less than 200 ppm.

The crystal structures of PHB and PHV have been reported by a very few authors.¹⁷⁻²⁰ There are surprisingly few published works on the physical properties of PHB^{21,22} and the new copolymer P(HB-HV).^{24,26} In the previous paper,²³ we reported the study on thermal analysis and lamellar thickening behavior of PHB and P(HB-HV) on annealing without solvent. Some thermodynamic constants of these polymers were proposed, and it was inferred that the HV component cannot crystallize at all, and does not have much effect upon the lattice indices of the crystal of HB component, but has a severe effect upon the crystallization characteristics of the copolymer. Bluhm *et al.*²⁴ have reported that for samples of HV content up to 30 mol%, HV units are accommodated in the PHB crystal lattice by a small lateral expansion of the unit cell, while the fiber repeat remains unchanged and they concluded the copolymers P(HB-HV) to be isomorphous.

In this paper we present details of our study of crystallization in a solvent, comparing with the results of the previous paper. Melting points and long spacings of these solution-grown crystals of PHB and its copolymer P(HB-HV) are studied and the morphology of them is examined by means of transmitting electron microscopy and structural change is estimated from the results of X-ray and electron diffractions. Since the biosynthetic process had a restriction of HV content in the bacterial copolymer less than 30 mol%, we can only discuss the influence of the minor (HV) component on the thermal behavior, structural change and morphology. From the experimental results, we can infer how the minor com-

ponent (HV) acts within the major component (HB).

EXPERIMENTAL

PHB and its copolymer used were the same specimens as those of the previous paper²³ supplied by ICI. The samples were semicrystalline powders that had been isolated from *Alcaligenes eutrophus* cultures and precipitated from chloroform solution by the addition of methanol.²⁵ The samples were dissolved in propylene carbonate (polymer concentration: 0.01%) at high temperature, then kept at constant temperature from 50°C to room temperature as the content of HV component increased from 0 mol% up to 30 mol%, to crystallize completely. Here, we use conventionally the same quoted compositions of HV content as the previous paper,²³ although the more reliable compositions²⁶ estimated from the NMR study may be considerably smaller than the quoted ones, whose study is reported elsewhere.²⁷ Then the solutions were heated up slowly to seed until at the temperature where their colour became transparent and successively put them into the oil bath at selected temperatures, kept constant to within $\pm 0.1^\circ\text{C}$. After isothermal crystallization for 24 h (both samples of 17 and 30 mol% HV contents were kept for a longer time up to a few weeks because of the extraordinary slow crystallization rate), it was filtered at that temperature and washed with methanol to remove the solvent completely. These single crystal mats were dried, then pressed to improve thermal conductivity and remove microvoids.

The melting behaviour of a 3 mg sample was studied in a Perkin Elmer differential scanning calorimeter DSC-II at a heating rate of 10 K min^{-1} under nitrogen atmosphere. Wide-angle and small-angle X-ray scatterings (WAXS and SAXS, respectively) were recorded photographically with the same conditions as the previous paper.²³ Electron microscopy

was studied putting the sample onto a micro-grid and for the image observation it was shadowed with Pt-Pd.

RESULTS AND DISCUSSION

DSC curves for the single crystal mats of PHB and its copolymers of 3, 8, and 10 mol% HV contents which were isothermally crystallized at 70°C are shown with curves (a–d), and those of copolymers of 17 and 30 mol% HV contents crystallized isothermally at 60 and 40°C are shown with curves (e) and (f) in Figure 1, respectively. All the samples of HV contents up to 10 mol% show two melting peaks at the lower and the higher temperatures. Both samples of 17 and 30 mol% HV showed a broader peak with a shoulder at the lower temperature. When it was measured with a wide range of heating rates from 0.31 to 80 K min⁻¹ the melting peak at the higher temperature shifted to the lower temperature and decreased in its area, while that at the higher temperature remained almost unchanged in peak temperature and area. This is because the peak appearing at the lower temperature corresponds to the melting peak of the original crystal of the sample crystallized isothermally, whereas that at the higher temperature is presumed to be mainly caused by the reorganized crystal²⁸ formed during the heating process. The melting peaks shift to lower temperatures and decrease in their peak areas as the HV content increases. For comparison, the broken lines in the figure show the DSC heating curves (2nd run) of each melt-quenched sample. Their melting peaks appear as almost single peaks. The melting points of melt-quenched samples agreed closely to those in the previous paper²³ which decreased according to the Flory equation for a random copolymer.²⁹ Bluhm *et al.*²⁴ have reported that these copolymers show steeper depression in melting points against more reliable compositions than the above ones, which also implies they are statistically random copolymers.

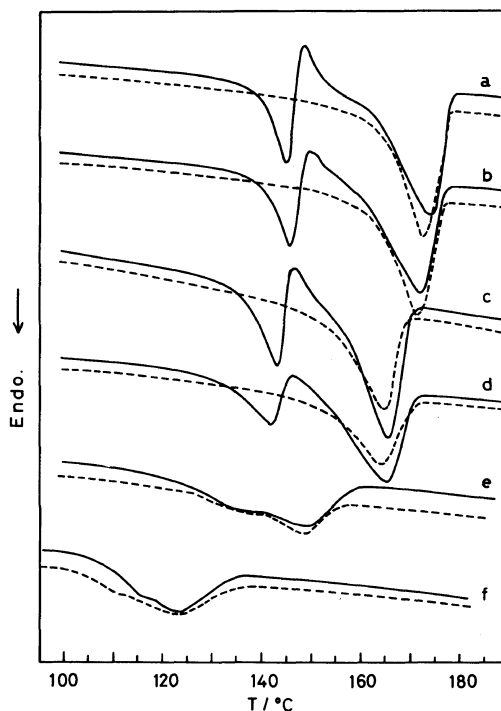


Figure 1. Typical DSC heating curves of single crystal mats of PHB and its copolymers P(HB-HV). (a), PHB; (b), 3 mol% HV content; (c), 8 mol% and (d), 10 mol% crystallized at 70°C for 24 h; (e), 17 mol% and (f), 30 mol% HV contents crystallized at 60°C and 40°C for 3 weeks, respectively. The broken lines show DSC heating curves of the respective samples melt-quenched.

Figure 2 shows DSC heating curves for the mats of PHB and its copolymer (10 mol% HV) crystallized at some high temperatures. The melting peak at the lower temperature shifts to the higher temperature and increases in its peak area as the crystallization temperature rises, whereas the one at the higher temperature is almost unchanged, but decreases in its peak area. This result also supports the assumption of reorganization.

The melting points (T_m) of solution-grown samples are plotted against the crystallization temperature (T_c) in Figure 3. PHB shows two series of melting points, the lower temperature series increases almost linearly (along the broken line) with increasing crystallization temperature, whereas the higher one is rather

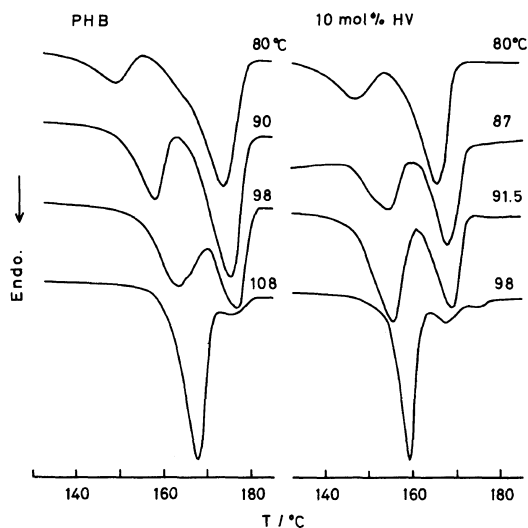


Figure 2. DSC heating curves for the mats of PHB and its copolymer (10 mol% HV content) crystallized at several high temperatures as shown in the figure.

unchanged. Since the latter series of the other samples appeared in a manner similar to that of PHB (*cf.* Figure 1), we omitted them here. The melting point series of the samples with HV contents of 3, 8 and 10 mol% shift to the slightly lower temperature (up to *ca.* 5°C) and increase almost parallel to that of PHB as the crystallization temperature rises. In the previous paper,²³ the melting points of all samples against annealing temperature were almost aligned on a line of PHB with a slope close to unity. In this study, the slope for samples crystallized isothermally in propylene carbonate, however, is smaller than unity, which means that the melting points increase more slowly against the crystallization temperature. The melting point series of samples of 17 and 30 mol% HV shift to the lower temperature *ca.* 10°C and decrease in their gradients with increasing HV content, reflecting rather incomplete crystallization of the HB component caused by some interruption of the HV component such as steric hindrance.

Figure 4 shows typical SAXS photographs of single crystal mats of PHB and P(HB-HV) (10 and 30 mol% HV contents) isothermally

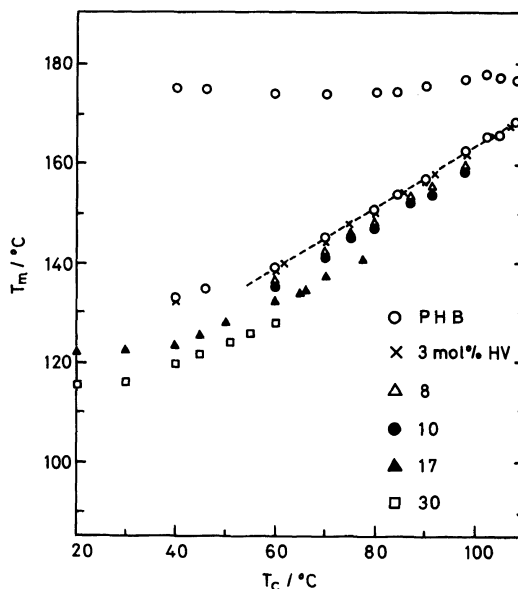


Figure 3. Melting points (T_m) of single crystal mats of PHB and P(HB-HV) crystallized at the crystallization temperature (T_c) as shown.

crystallized at several temperatures. Long spacings of all samples are plotted against crystallization temperatures in Figure 5. The sample shows a hyperbolic curve which shifts to the lower temperature as the HV content increases. In the previous paper,²³ the annealed samples showed discontinuous hyperbolic curves accompanied by jumping steps in temperature ranges where the exothermic peaks appeared (*cf.* Figure 1). In these temperature ranges, the samples showed two long spacings, an original long spacing and a thicker one nearly double the original. This implies that the original crystal is difficult to thicken smoothly, but can suddenly increase in its thickness nearly double the original one. On the contrary, the solution-grown samples usually show only one long spacing. Since the copolymers were crystallized in the solution more slowly and completely, they show smoother lamellar thickening curves and less band broadening in SAXS patterns.

The equilibrium melting point T_m° estimated by the annealing without solvent was pro-

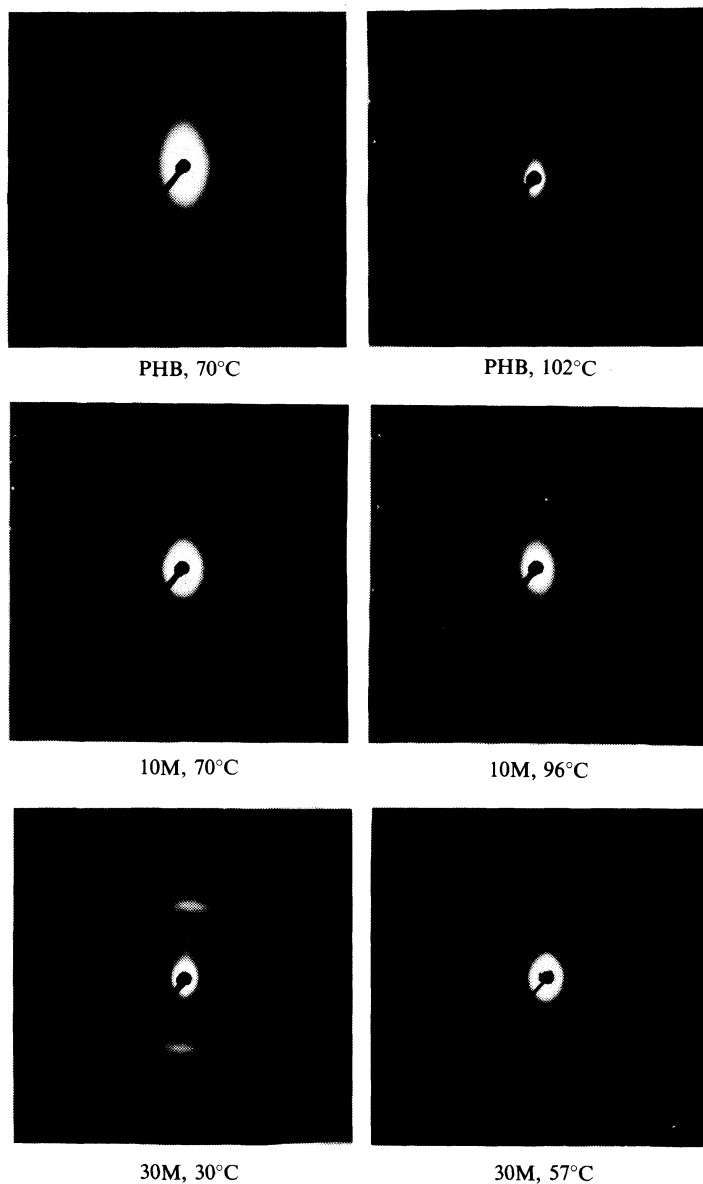


Figure 4. Typical SAXS photographs of single crystal mats of PHB and P(HB-HV) (10 and 30 mol% HV contents) crystallized at several temperatures as shown.

posed²³ (e.g., 197°C for PHB and 143°C for sample of 30 mol% HV content), which closely agreed with T_m° evaluated for solution-grown samples, though this is uncertain because the long spacings against crystallization temperatures varied in the range (4.4–9.4 nm) narrower than the former case. We

cannot estimate T_m° in a propylene carbonate solution from the seeding temperature,³⁰ but can make a rough estimate as the temperature (T_c) where the T_m° intersects an extension line of the T_m-T_c curve in Figure 3 (assuming T_m-T_c curve to be linear to higher temperatures) as follows; PHB, 155°C; 3 mol%

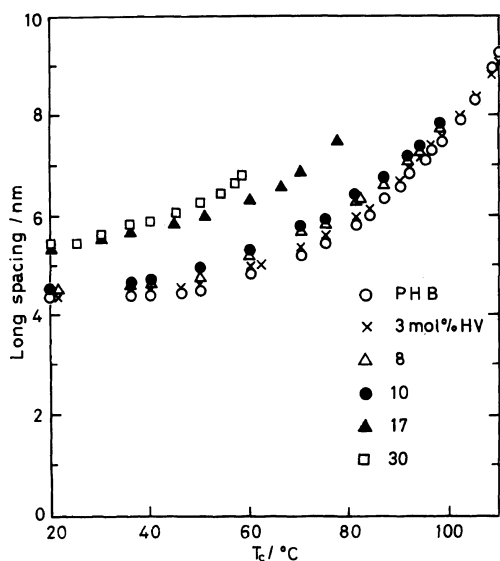


Figure 5. Long spacings of single crystal mats of PHB and P(HB-HV) crystallized at the crystallization temperatures (T_c).

HV content, 151°C; 8 mol%, 145°C; 10 mol%, 140°C; 17 mol%, 122°C; and 30 mol%, 95°C. As shown in Figure 5, we might roughly say that all curves of PHB and P(HB-HV) of HV content up to 10 mol% can be superposed on each other, shifting by the supercooling temperature ΔT which equals to $T_m^0 - T_c$ for the most part, except for the higher temperature range, while those of samples of 17 and 30 mol% HV show inferior superposition. As the HV content increases, the deviation from the PHB curve becomes larger and the rate of increase and the maximum of long spacing become lower.

Figure 6 shows typical electron micrographs of single crystals of PHB and its copolymer (3 mol% HV) crystallized at several high temperatures. Some of us have already reported the morphologies of PHB single crystals grown at lower temperatures (36–83°C). The crystals always appear to have an elongated arrow-like shape, although the edges are often quite rough (particularly at lower crystallization temperatures). In some cases, the crystals appear to have a three-dimensional tent-like

structure. PHB single crystals grown at 84°C show large arrow-like crystals with relatively smooth edges or sides, and a saw-toothed short edge is sometimes observed in place of the apex of the crystal. The maximum growth rate of crystallization in propylene carbonate seems to be at temperature range around 60–70°C, while that of spherulite without solvent was around 80–90°C²¹. Therefore, predominant growth along the long axis becomes less as the crystallization temperature increases (above *ca.* 80°C), which results in reduction in crystal size and change into rather lath or oblong shapes with inclined short sides like a sword. The morphology of the sample with 3 mol% HV content essentially shows the trend similar to that of PHB.

Figure 7 shows electron micrographs of the samples of the other HV contents (8–30 mol% HV). The lath-like crystals slightly decrease in size until the HV content increases to around 10 mol%, although the morphological characteristics are very similar to PHB. Both samples of 17 and 30 mol% HV contents show very irregular and small crystals. The sample of 30 mol% HV content grown at room temperature shows small arrow-shaped crystals, while that grown at 51°C shows relatively larger and thicker crystals with somewhat bumpy surfaces. It is conceivable that it is difficult for the HV component to penetrate the HB component crystals because the bulkier side group of HV component causes steric hindrance. However, it is impossible to prevent some HV units in the copolymer chain from penetrating the HB crystals by degrees as the HV content increases, which causes the lattice strain or distortion in HB crystals and results in the morphological irregularity during the crystallization. Consequently, both samples of 17 and 30 mol% HV contents grown at high temperatures show fibrillar or lath shaped crystals with bumpy surfaces.

There are few reports concerning the crystal structures of PHB and PHV. The unit cells of PHB and PHV are orthorhombic, $P2_12_12_1-D^4_2$,

Crystallization and Morphology of PHB and Its Copolymer

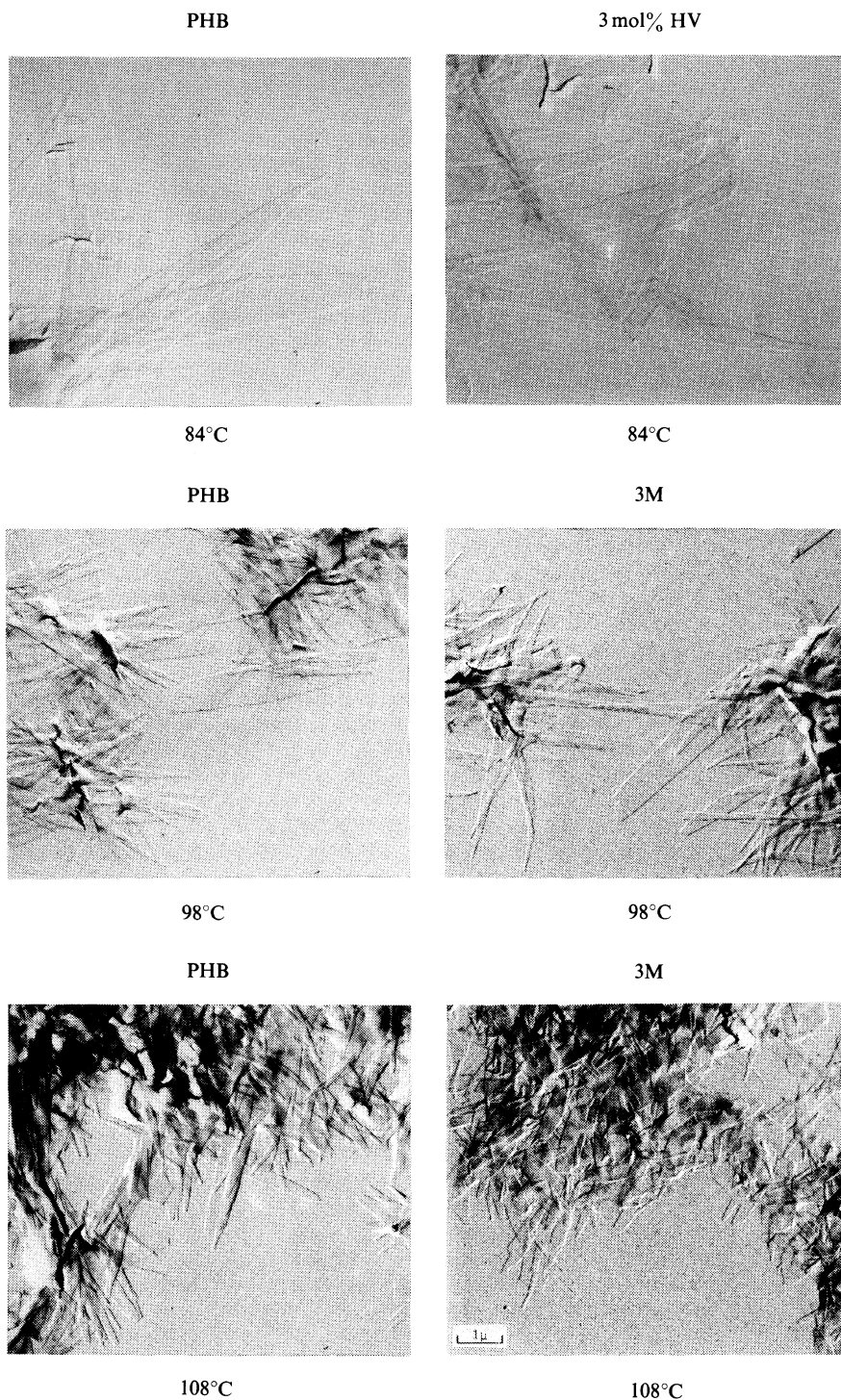
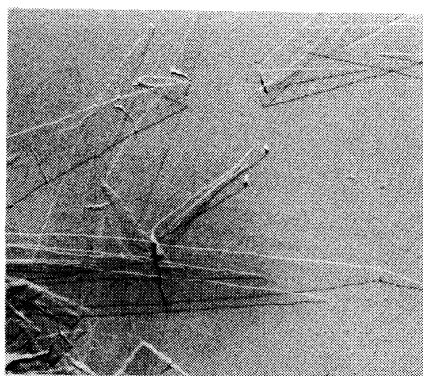
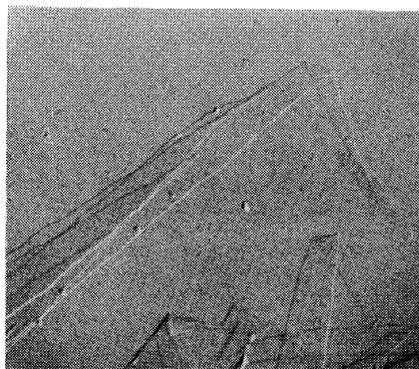


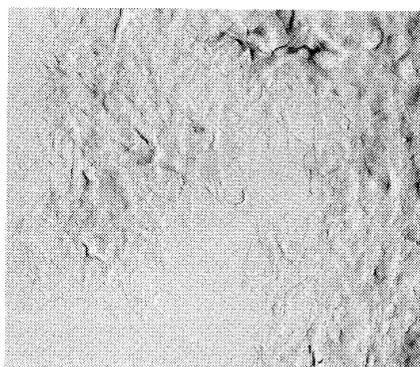
Figure 6. Typical electron micrographs of single crystals of PHB and the copolymer of 3 mol% HV content crystallized at some high temperatures as shown.



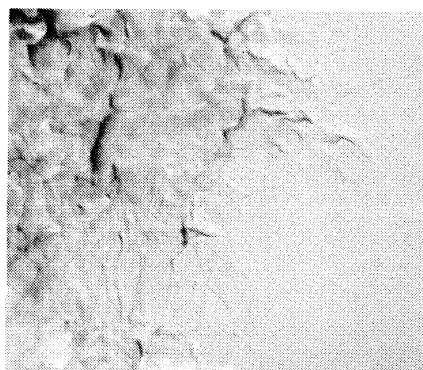
8M, 75°C



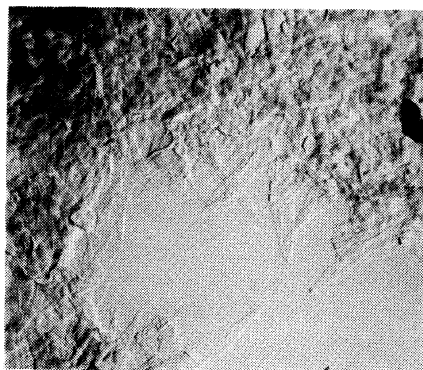
10M, 75°C



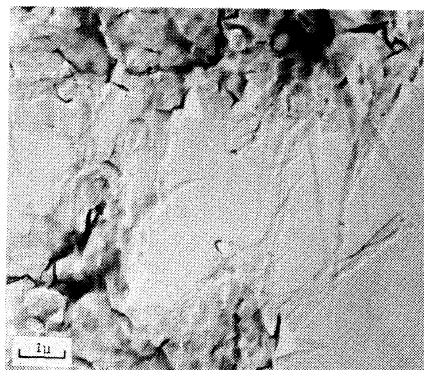
10M, 85°C



17M, 70°C



30M, 20°C



30M, 51°C

Figure 7. Typical electron micrographs of single crystals of the copolymers of 8, 10, 17, and 30 mol% HV contents at some different temperatures as shown.

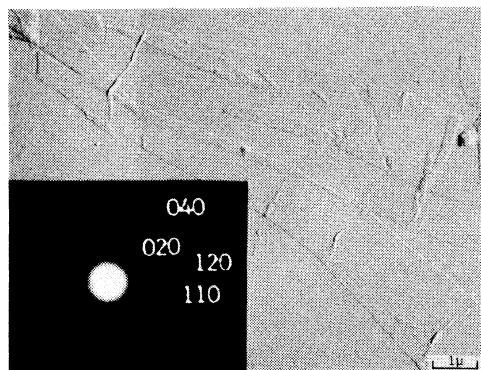


Figure 8. Electron micrograph of PHB single crystal crystallized at 70°C with its electron diffraction pattern showing the indexing of the spots inset.

with $a=5.76 \text{ \AA}$, $b=13.20 \text{ \AA}$, and c (fiber period) $=5.96 \text{ \AA}$ for PHB¹⁸ and $a=9.52 \text{ \AA}$, $b=10.08 \text{ \AA}$, and c (fiber period) $=5.56 \text{ \AA}$ for the naturally occurring PHV and two molecules giving a left-handed (2/1) helix pass through the unit cell.³¹ PHB crystals of synthesized racemic polymer give the same X-ray and electron diffraction patterns as that of a naturally occurring polymer; however, PHV crystals of racemic polymers give smaller a parameter.³² Figure 8 shows an electron micrograph of the PHB single crystal crystallized at 70°C with its electron diffraction pattern with the indexes of the spots. Selected area electron diffraction from part of a crystal indicates that the crystallographic a -axis runs along the long direction of each crystal and the b -axis is perpendicular to the long axis and the c -axis is normal to the substrate. The short edge or side inclined to the long axis is frequently observed for samples grown at higher temperatures, which is supposed to correspond to the (110) plane, while the long sides closely correspond to the (010) plane. However, if the angle of apex of the arrow becomes larger and the long sides deviate from the parallelism at relatively low temperatures (below *ca.* 70°C), the sides or edges along the long axis become rough or saw-toothed (probably alternately composed of

two main planes of (110) and (010)). Two of us have suggested from the observation of the stretched PHB single crystal that the chains apparently fold parallel to the long axis of the crystals, the crystallographic a -axis.²¹ Moreover, we can frequently observed square or polygonal shaped crystals for the samples crystallized at higher temperatures (*e.g.*, 3 mol% HV (108°C) and 10 mol% (85°C) in Figure 6 and 7). This implies that the predominant growth along a -axis becomes less and gradually comparable with that along the b -axis as the crystallization temperature increases.

Figure 9 shows typical electron diffraction patterns of some copolymers. The spotted diffraction pattern of PHB or 3 mol% HV changes into the arc-like one composed of the aggregation of many spots diffracted from the smaller crystals as the HV content increases, finally showing almost complete rings for the sample of 30 mol% HV content. The arc-like pattern is caused by change in orientation of crystals overlapped each other. Besides, the samples of high HV content (*i.e.*, 17 and 30 mol% HV) show line broadening of the arc, which is caused by reduction in crystal size and introduction of irregularity. However, there are no essential difference in the spacings of spots or arcs even for the sample of 30 mol% HV content. Bluhm *et al.*²⁴ have reported that d spacings from X-ray fiber diffraction diagrams indicate an expansion of the (110) plane of the PHB lattice, while the (020) and (002) d spacings are unchanged, leading to the conclusion that only the a parameter of the unit cell changes, *i.e.*, it increases almost linearly from 5.76 Å (PHB) to 5.96 Å (20 mol%) and 6.05 Å (29 mol%). We can recognize similar expansion of the (110) plane, from which is evaluated the slightly smaller increase in a parameter to 5.76 Å (PHB), 5.78 Å (3 mol% HV), 5.80 Å (8 mol%), 5.81 Å (10 mol%), 5.85 Å (17 mol%) and 5.90 Å (30 mol%). The (020) spacing of the copolymers coincides strictly with that of PHB crystal.

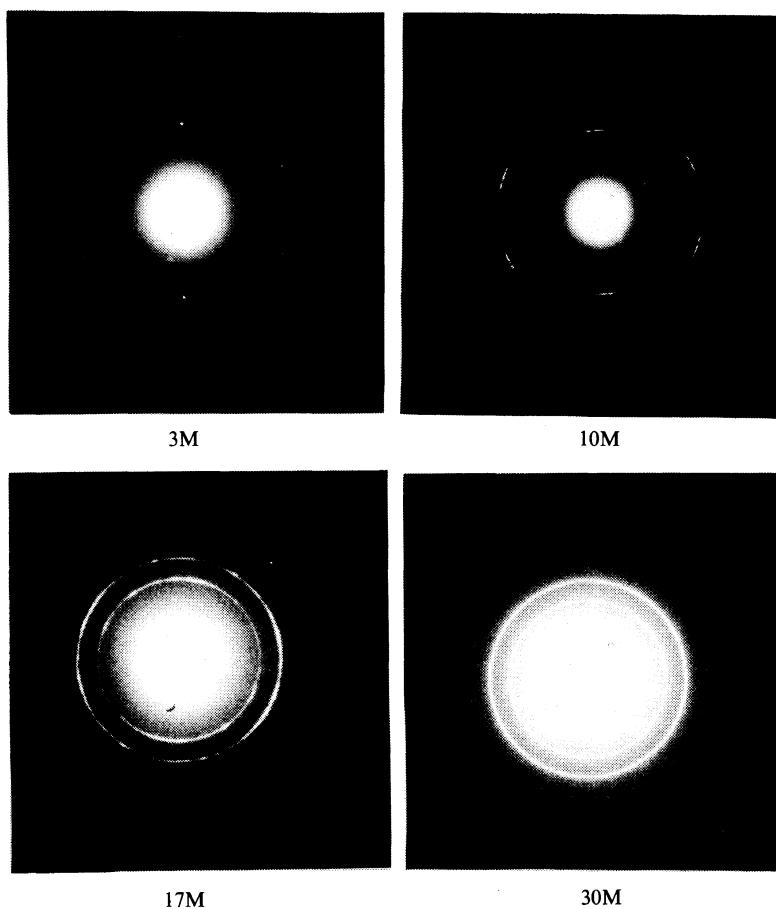


Figure 9. Typical electron diffraction patterns of the copolymers of 3, 10, 17, and 30 mol% HV contents.

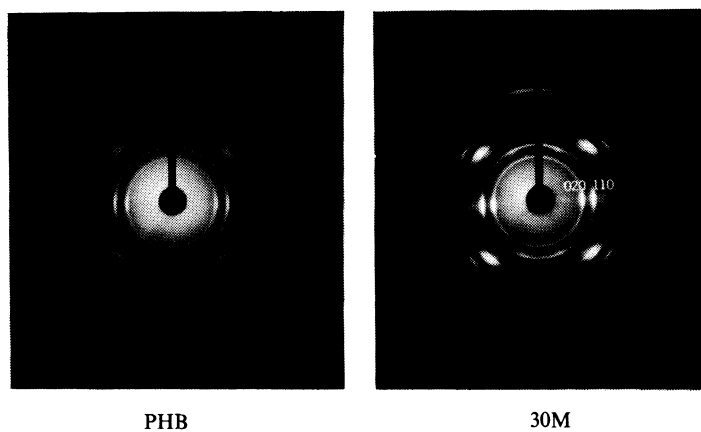


Figure 10. WAXS fiber diagrams of PHB and the copolymer of 30 mol% HV content (hot drawn) showing the indexing of (020) and (110) spots.

This implies that the only HB component can crystallize. On the other hand, the HV component cannot crystallize in it, but remains non-crystalline and acts as a defect because the HV unit is copolymerized in a random manner in the polymer chain.²³

Figure 10 shows WAXS fiber diagrams of solution-grown samples of PHB and the copolymer of 30 mol% HV content showing the indexing of (020) and (110) spots. They were obtained by hot drawing to about five (PHB) to ten (30 mol%) times the original length at temperatures just below the melting points (highly oriented along *c*-axis). We can conclude that there are no changes in the (020) and (002) *d* spacings, and small expansion of (110) *d* spacing, closely paralleling the results of electron diffractions. The *a* parameter estimated from WAXS fiber diagrams increased linearly as follows; 5.76 Å (PHB), 5.77 Å (3 mol% HV), 5.79 Å (8 mol%), 5.80 Å (10 mol%), 5.84 Å (17 mol%), and 5.89 Å (30 mol%). The expansion of a unit cell for the solution-grown samples undrawn is very similar to that of the hot drawn samples. We could also find very similar variation for the other samples having the more reliable HV content of 20% and 26%, whose *a* parameters are 5.87 Å and 5.95 Å, respectively. Bluhm *et al.*²⁴ have proposed that the melting point vs. composition curve shows an eutectic-like behavior and has the minimum point at a composition near 30 mol% HV units, and that only the PHB crystal phase appears below the HV content than this point, and the PHV crystal phase does above it. Consequently they supposed these copolymers are isodimorphic. We could confirm the above presumption for copolymers at lower HV contents. However, the HV units are inclined to be excluded outwards as much as possible during the crystallization, which results in the expansion of the HB crystal slightly smaller than that of solution-cast films as reported by them.²⁴

In conclusion, it is inferred that the naturally occurring P(HB-HV) copolymers have

a statistically random distribution of comonomer units.^{26,27} The equilibrium melting points of copolyesters decreased according to the Flory's equation for a random copolymer^{23,24} irrespective of sample preparations. All the solution-grown samples showed only one melting peak in DSC curves and a diffused SAXS diffraction, which implies that these copolymers have only a single crystalline phase of the HB component. Melting points of the solution-grown samples increased linearly against crystallization temperatures, however, the slope became gentler as the HV content increased. Long spacings of them increased hyperbolically, but the rate of increase and the maxima of long spacings also decreased as the HV content increased. These results reflect incomplete crystallization caused by some interruption of the HV component such as steric hindrance. Crystallinity of the sample steeply decreased with increasing the HV content²³ (*cf.* Figure 1).

Single crystals of PHB grown at the lower temperature showed the elongated arrow-like crystal with rough edges. They changed into the lath or elongated oblong shape with quite smooth edges (frequently accompanied by inclined short sides) when grown at the higher temperature. The copolymer of HV contents less than 10 mol% showed the similar trend in the morphological variation to that of PHB. However, the remarkable changes such as reduction in crystal size and introduction of irregularity are observed at the high HV content more than 10 mol% (*i.e.*, 17 and 30 mol%). The HV component in the copolymer chain is inclined to be excluded outwards as much as possible from the crystal of HB component during the crystallization. For this reason, the fold surface or boundary of the crystal becomes more irregular (and probably thicker) as the HV content increases, which causes a steep decrease in the rate of crystallization and incomplete lamellar thickening. It also results in strong restriction of further lamellar thickening at higher crystallization

temperatures.

We could find only a single crystal phase of the HB component by electron and X-ray diffractions. Small expansion of only the a parameter of the unit cell is observed with increasing the HV content, which is caused by the occlusion of the HV units in the HB crystal. However, solution-grown samples showed the expansion slightly smaller than that as reported for solution-cast films,²⁴ which also supports the presumption that the HV units are inclined to be excluded outwards from the HB crystal. We can make a rough estimate for all samples that the mole fraction of HV units within the HB crystal is about half the initial mole fraction, assuming the lateral expansion of the unit cell caused by the difference between the volumes of HB (453.2 \AA^3) and HV (533.5 \AA^3) units (probably, both units took laterally distorted postures).³¹ This is somewhat overestimated because the HV unit can not exist as crystalline phase in HB crystals, though further study is needed to explain this more precisely. Some HV units are statistically occluded and act as defects in the HB crystals, which do not have much effect on the lattice dimension (only the a parameter increases slightly), but cause the lattice strain. They result in significant depression in the melting point, the heat of fusion of the HB component crystal²⁴ and the fold surface free energy.²³

Acknowledgement. We thank Dr. David J. Brown, Biological Products Business in Imperial Chemical Industries PLC for supplying us with the specimens and Dr. R. H. Marchessault, Vice-President of Xerox Research Centre of Canada, for his many helpful comments through private letters.

REFERENCES

1. M. Lemoigne, *Ann. Inst. Past.*, **39**, 144 (1925).
2. J. Merrick, *Photosynth. Bact.*, **199**, 219 (1978).
3. E. A. Dawes and P. J. Senior, *Adv. Microbial Phys.*, **10**, 138 (1973).
4. J. S. Herron, J. D. King, and D. C. White, *Appl. Environ. Microbiol.*, **35**, 251 (1978).
5. N. G. Carr, *Biochem. Biophys. Acta*, **120**, 308 (1966).
6. L. L. Wallen and W. K. Rohwedden, *Environ. Sci. Technol.*, **8**, 576 (1974).
7. A. C. Ward, B. I. Rowley, and E. A. Dawes, *J. Gen. Microbiol.*, **102**, 61 (1977).
8. D. G. Lundgren, R. Alper, C. Schnaitman, and R. H. Marchessault, *J. Bacteriol.*, **89**, 245 (1965).
9. P. A. Holmes, L. F. Wright, and B. Alderson, Eur. Patent Appl., 15123 (1979).
10. J. N. Baptist, US Patent, 3044942 (1962).
11. J. N. Baptist, US Patent, 3036959 (1962).
12. R. M. Lafferty, *Chem. Rundsch.*, **30**, 15 (1977).
13. E. R. Howells, *Chem. Ind.*, 508 (1982).
14. R. H. Marchessault, *CHEMTECH*, 542 (1984).
15. J. B. Cragi, D. R. Lloyd, Proceedings of CHEMRAWN III Conference, The Hague, 1984, IUPAC, Section 3 IV, "Alternative Carbon Sources."
16. P. A. Holmes, L. F. Wright, and S. H. Collins, Eur. Patent Appl., 0052459 (1981); Eur. Patent Appl., 0069497 (1981).
17. J. Combard and R. H. Marchessault, *J. Mol. Biol.*, **71**, 735 (1972).
18. M. Yokouchi, Y. Chatani, H. Tadokoro, K. Teranishi, and H. Tani, *Polymer*, **14**, 267 (1973).
19. K. Okamura and R. H. Marchessault, "Conformational Aspects of Biopolymers," Vol. II, G. N. Ramachandran, Ed., Academic Press, London and New York, 1967.
20. R. H. Marchessault, S. Coulombe, H. Morikawa, K. Okamura, and J. F. Revol, *Can. J. Chem.*, **59**, 38 (1981).
21. P. J. Barham, A. Keller, E. L. Otun, and P. A. Holmes, *J. Mater. Sci.*, **19**, 2781 (1984).
22. P. J. Barham, *J. Mater. Sci.*, **19**, 3826 (1984).
23. H. Mitomo, P. J. Barham, and A. Keller, *Sen-i Gakkaishi*, **42**, T-589 (1986).
24. T. L. Bluhm, G. K. Hamer, R. H. Marchessault, C. A. Fyfe, and R. P. Veregin, *Macromolecules*, **19**, 2871 (1986).
25. P. A. Holmes, L. F. Wright, and S. H. Collins, Eur. Patent Appl., 0052459 (1982); Eur. Patent Appl., 0069497 (1983).
26. S. Bloembergen, D. A. Holden, G. K. Hamer, T. L. Bluhm, and R. H. Marchessault, *Macromolecules*, **19**, 2865 (1986).
27. H. Mitomo and T. Takizawa, *Sen-i Gakkaishi* (to be published).
28. T. Arakawa, F. Nagatoshi, and N. Arai, *J. Polym. Sci., Polym. Lett.*, **6**, 513 (1968); *J. Polym. Sci., Polym. Phys. Ed.*, **7**, 1461 (1969).
29. P. J. Flory, *J. Chem. Phys.*, **17**, 223 (1949).
30. H. Mitomo and A. Keller, *Rep. Prog. Polym. Phys. Jpn.*, **29**, 153 (1986).

Crystallization and Morphology of PHB and Its Copolymer

31. R. H. Marchessault, H. Morikawa, J. F. Revol, and T. L. Bluhm, *Macromolecules*, **17**, 1884 (1984).
32. M. Yokouchi, Y. Chatani, H. Tadokoro, and H. Tani, *Polymer J.*, **6**, 248 (1974).